JOURNAL OF CHEMICAL & ENGINEERING DATA

ARTICLE

pubs.acs.org/jced

Molar Heat Capacities, Thermodynamic Properties, and Thermal Stability of $Lu(C_2H_5O_2N)_2Cl_3 \cdot 3H_2O$

Xue-Chuan Lv,[†] Zhi-Cheng Tan,[*,‡,§] and Xiao-Han Gao[†]

[†]School of Chemistry and Material Science, Liaoning Shihua University, Fushun 113001, China

[‡]China Ionic Liquid Laboratory and [§]Thermochemistry Laboratory, Dalian Institute of Chemical Physics, Chinese Academy of Sciences, Dalian 116023, China

ABSTRACT: A complex of lutetium hydrochloric acid coordinated with 2-aminoacetic acid ($C_2H_5O_2N$), $Lu(C_2H_5O_2N)_2Cl_3 \cdot 3H_2O$, was synthesized. The molar heat capacities ($C_{p,\mathrm{m}}$) and thermodynamic properties of the complex were studied with an automatic adiabatic calorimeter from (80 to 373) K. The thermodynamic functions $[H_T - H_{298.15\mathrm{K}}]$ and $[S_T - S_{298.15\mathrm{K}}]$ were derived over the temperature range from (85 to 315) K with a temperature interval of 5 K. The thermal decomposition behavior of the complex under a nitrogen atmosphere was studied by thermogravimetric analysis, differential thermal analysis, and differential scanning calorimetry.

INTRODUCTION

Rare-earth elements have many unique biochemical properties. With the great progress being made in cognition and research on the complexes of rare-earth ions with amino acids, the complexes have been used in many areas, such as fertilizers, pesticides, antibacterial agents, and so on. It is undoubtly the case that rare-earth elements would inevitably be spread into the bodies of beings with their applications. Therefore, it is necessary to obtain information about the long-term effects of rare-earth elements on people and explore more extensive applications of the complexes. Up to now, the complexes of lanthanide ions with amino acids have been synthesized and studied by a variety of methods.[1−5] However, only a few publications have dealt with the thermodynamic properties,[6,7] such as the molar heat capacity ($C_{p,\mathrm{m}}$).

The values of $C_{p,\mathrm{m}}$ for a compound as a function of temperature are basic physical data. From these data, many other thermodynamic properties, such as enthalpy, entropy, and Gibbs free energy, can be calculated,[8] and these thermodynamic properties are important for both theoretical and practical purposes. Adiabatic calorimetry at temperatures from below 1 K to those approaching the limits imposed by the materials themselves[8] is a classical method for heat capacity measurements.

In the present investigation, a low-temperature adiabatic calorimeter for small samples, whose structure, working principle, and reliability have been described in our previous works,[6−13] was used to measure $C_{p,\mathrm{m}}$ for the title compound, $Lu(C_2H_5O_2N)_2Cl_3 \cdot 3H_2O$. The thermodynamic properties of the complex were studied using differential scanning calorimetry (DSC) and thermogravimetric and differential thermal analysis (TG−DTA).

EXPERIMENTAL SECTION

Synthesis and Characterization of the Complex. $Lu(C_2H_5O_2N)_2Cl_3 \cdot 3H_2O$ was synthesized by a previously reported procedure.[14] The rare-earth oxide (Lu_2O_3) was dissolved in an excess amount of hydrochloric acid, and the concentration of the solution was determined by EDTA titration analysis. Next, solid 2-aminoacetic acid ($C_2H_5O_2N$) was added to the solution of Lu^{3+} in a Lu^{3+}:$C_2H_5O_2N$ molar ratio of 1:2. The pH of the reaction mixture was carefully adjusted to ~2.5 by slow addition of NaOH solution. The mixture was stirred at 333 K in A water bath for (7 to 8) h. The solution was then condensed at room temperature for 2 weeks, and crystals were obtained. The crystals were washed with anhydrous ethanol three times and placed in a desiccator filled with phosphorus pentoxide. The purity of the crystals was proved by EDTA titrimetric analysis to be greater than 0.999 mass fraction, which was sufficient to meet the requirements of the present calorimetric study.

IR spectra of the complex and 2-aminoacetic acid were obtained at room temperature using a Bruker Tensor 27 IR spectrophotometer with KBr pellets. Compared with the IR spectrum of 2-aminoacetic acid, the peak of the $\nu_s(\mathrm{COO}^-)$ band of the complex shifted from 1412 cm^{-1} to higher wavenumbers (1419 cm^{-1}), the special absorptions of ν_{as}-(COO^-) shifted from (1591 to 1620) cm^{-1}, and the ω-(COO^-) absorption moved from (607 to 592) cm^{-1}, showing that the carboxyl groups of the ligand were coordinated to the metal ion.[15] In the spectrum, the $\delta(\mathrm{NH}^{2+})$ absorption peak shifted from (1521 to 1538) cm^{-1}. A broad absorption band for $\nu(\mathrm{OH})$ appearing at 3418 cm^{-1} showed the presence of water molecules in the complex.

Adiabatic Calorimetry. A precision automatic adiabatic calorimeter was used to measure $C_{p,\mathrm{m}}$ for the complex over the temperature range from (80 to 373) K. The calorimeter was

Special Issue: John M. Prausnitz Festschrift

Received: October 30, 2010
Accepted: February 23, 2011
Published: March 11, 2011

Table 1. Experimental Molar Heat Capacities ($C_{p,\mathrm{m}}$) of α-Al_2O_3 (M = 101.96 g·mol^{-1})

T	$C_{p,\mathrm{m}}$	T	$C_{p,\mathrm{m}}$	T	$C_{p,\mathrm{m}}$
K	J·K^{-1}·mol^{-1}	K	J·K^{-1}·mol^{-1}	K	J·K^{-1}·mol^{-1}
78.64	6.377	159.7	35.90	280.2	74.99
79.62	6.725	163.4	37.37	283.6	76.00
80.91	7.105	166.9	38.84	287.0	76.62
82.61	7.649	170.4	40.20	289.8	77.23
84.26	8.043	173.9	41.46	292.7	78.02
85.87	8.526	177.2	42.75	295.4	78.49
87.44	9.002	180.5	43.99	298.1	79.02
88.97	9.467	183.8	45.19	301.3	79.65
90.47	9.920	186.9	46.44	304.5	80.50
91.93	10.37	190.1	47.59	307.2	80.95
93.37	10.81	193.2	48.72	309.9	81.50
94.78	11.26	196.6	49.96	312.6	82.03
96.16	11.72	200.3	51.29	315.2	82.53
97.52	12.18	204.0	52.56	317.9	83.03
98.86	12.63	207.7	53.87	320.5	83.48
100.2	13.07	211.3	55.06	323.5	84.11
101.5	13.50	214.8	56.28	326.9	84.73
102.7	13.95	221.7	58.48	330.2	85.33
104.0	14.44	225.1	59.62	333.5	86.15
106.6	15.36	228.4	60.72	336.8	86.67
110.5	16.76	231.7	61.72	340.7	87.33
114.2	18.09	234.9	62.69	345.1	88.15
120.0	20.09	238.1	63.68	349.5	88.83
120.9	20.67	241.3	64.57	353.9	89.56
123.1	21.59	244.5	65.50	358.2	90.25
126.3	22.85	247.6	66.49	362.4	90.73
129.5	24.08	250.7	67.28	366.7	91.61
132.6	25.30	253.7	68.20	370.8	92.38
135.6	26.49	256.8	69.05	375.0	93.16
138.6	27.65	259.8	69.87	378.9	93.55
141.4	28.77	262.8	70.67	383.0	94.01
144.3	29.85	265.8	71.44	387.4	94.61
147.3	31.01	268.7	72.19	391.8	95.13
149.3	32.04	271.6	72.94	396.2	95.74
152.5	33.27	274.5	73.67	400.4	96.18
156.0	34.69	277.4	74.36		

established in the Thermochemistry Laboratory of the Dalian Institute of Chemical Physics, Chinese Academy of Sciences.

The structure and principle of the adiabatic calorimeter have been described in detail elsewhere.[8−13] The automatic adiabatic calorimeter consisted of a sample cell made of gold-plated copper; a miniature platinum resistance thermometer (IPRT no. 2, produced by Shanghai Institute on Industrial Automatic Meters; 16 mm in length, 1.6 mm in diameter, and a nominal resistance of 100 Ω); an electric heater; the inner and outer adiabatic shields; two sets of six-junction chromel—constantan thermopiles, one installed between the calorimetric cell and the inner shield and the other between the inner and outer shields; and a high-vacuum can.

Table 2. Comparison of Experimental Molar Heat Capacities ($C_{p,\mathrm{m}}$) of α-Al_2O_3 with the Values Recommended by NIST

	$C_{p,\mathrm{m}}$/J·K^{-1}·mol^{-1}				$C_{p,\mathrm{m}}$/J·K^{-1}·mol^{-1}		
T/K	present	NIST	δ^a/%	T/K	present	NIST	δ^a/%
80	6.901	6.90	0.01	250	67.08	67.06	0.03
90	9.678	9.67	0.08	260	69.82	69.80	0.03
100	12.85	12.84	0.08	270	72.42	72.41	0.01
110	16.34	16.34	0.00	280	74.87	74.88	−0.01
120	20.07	20.07	0.00	290	77.20	77.23	−0.04
130	23.95	23.95	0.00	300	79.41	79.45	−0.05
140	27.93	27.93	0.00	310	81.51	81.56	−0.06
150	31.95	31.94	0.03	320	83.49	83.55	−0.07
160	35.95	35.94	0.03	330	85.37	85.44	−0.08
170	39.90	39.89	0.03	340	87.16	87.23	−0.08
180	43.75	43.74	0.02	350	88.84	88.92	−0.09
190	47.50	47.50	0.00	360	90.45	90.52	−0.08
200	51.12	51.12	0.00	370	91.97	92.04	−0.08
210	54.61	54.61	0.00	380	93.41	93.48	−0.07
220	57.95	57.95	0.00	390	94.91	94.84	0.07
230	61.14	61.14	0.00	400	96.18	96.14	0.04
240	64.18	64.17	0.02				

[a] $\delta = (100\ \%)\cdot(C_{p,\mathrm{m,present}} - C_{p,\mathrm{m,NIST}})/C_{p,\mathrm{m,NIST}}$.

The effective capacity of the sample cell was 6 cm^3. Four gold-plated copper vanes with a thickness of 0.2 mm were placed inside with an X shape to promote heat distribution. The miniature platinum thermometer was inserted into a horizontal copper sheath soldered under the bottom. The thermometer was calibrated on the basis of ITS-90 by the Station of Low-Temperature Metrology and Measurements, Academia Sinica. The resistance of the thermometer was measured by a $7^1/_2$ digit NanoVolt/Micro-Ohm meter (model 34420, Agilent, USA). The heater wire was bifilarly wound and fixed around the outside wall of the sample cell. After the sample was loaded, the cell was sealed and evacuated. A small mount of helium gas (0.1 MPa) was introduced into the cell to enhance heat transfer.

The temperature difference between sample cell and inner shield and that between the inner and outer shields were monitored by two sets of thermocouples. Both shields were heated under the control of a temperature controller (model 340, Lakeshore, USA) and kept at the same temperature as the sample cell. The electrical energy introduced into the sample cell was automatically measured by a data acquisition/switch unit (model 34970A, Agilent). The equilibrium temperature of the cell after the energy input was measured using the $7^1/_2$ digit Nano Volt/Micro-Ohm meter. The energy and the temperature data were processed online by a computer.

The heat capacity measurements were conducted using the standard procedure of intermittently heating the sample and alternately measuring the temperature. The heating rate was (0.1 to 0.4) K·min^{-1}, and the temperature increments of the experimental points were between (1 and 4) K. The heating duration was 10 min, and the temperature drift rates of the sample cell, which were measured in an equilibrium period, were kept within (10^{-3} to 10^{-4}) K·min^{-1}.

The reliability of the newly constructed calorimetric system was verified by measuring the molar heat capacities of synthetic sapphire (α-Al_2O_3, Standard Reference Material 720). The results are listed in Table 1. In order to compare the values to

Table 3. Experimental Molar Heat Capacities ($C_{p,\mathrm{m}}$) of the Complex from (80 to 373) K

T	$C_{p,\mathrm{m}}$	T	$C_{p,\mathrm{m}}$	T	$C_{p,\mathrm{m}}$
K	$\mathrm{J \cdot K^{-1} \cdot mol^{-1}}$	K	$\mathrm{J \cdot K^{-1} \cdot mol^{-1}}$	K	$\mathrm{J \cdot K^{-1} \cdot mol^{-1}}$
82.23	257.6	184.6	525.9	286.4	666.5
86.90	268.7	187.6	531.3	289.4	669.1
89.64	277.0	190.5	539.3	292.3	671.7
92.54	284.9	193.5	544.2	295.3	676.8
95.58	294.6	196.6	550.7	298.5	681.2
98.76	305.3	200.1	557.2	301.6	683.6
101.9	313.7	203.3	562.1	304.6	688.1
104.9	321.2	206.4	566.3	307.8	689.3
107.8	330.2	209.6	572.8	310.9	696.7
110.7	339.6	212.7	577.3	314.1	706.3
113.8	348.0	215.8	582.3	317.0	712.9
117.0	356.4	218.7	588.8	320.1	722.5
120.1	365.8	221.7	592.2	323.4	731.7
123.2	374.6	224.7	598.3	326.5	744.0
126.2	383.4	227.8	602.5	329.6	758.7
129.2	392.5	230.8	607.4	332.6	772.2
132.1	399.7	233.9	612.8	335.7	787.5
135.2	408.6	237.1	616.2	338.7	804.8
138.4	415.8	240.2	621.9	341.7	822.9
141.6	424.2	243.2	625.4	344.7	841.8
144.7	432.6	246.4	629.1	347.7	864.5
147.8	440.9	249.5	632.2	350.9	891.1
150.9	448.2	252.7	635.2	354.0	921.1
153.9	453.9	255.8	638.2	357.1	951.3
156.9	460.7	258.9	642.2	360.2	980.6
159.9	469.1	262.0	644.7	363.2	1013
162.8	478.1	265.1	648.2	366.2	1049
165.9	485.5	268.1	651.2	369.2	1092
169.1	493.2	271.2	653.1	372.2	1146
172.3	499.3	274.3	656.2		
175.4	507.6	277.3	658.4		
178.5	514.2	280.3	659.9		
181.5	521.0	283.4	663.0		

those recommended by NIST,[16] the molar heat capacities of α-Al_2O_3 over the temperature range from (80 to 400) K with an interval of 10 K were calculated using the nonlinear insert method and the measured molar heat capacity data. The results are shown in Table 2. It can be seen from the table that the deviations of the present values from the recommended values are within ± 0.1 %.

In the present paper, the mass of $\mathrm{Lu(C_2H_5O_2N)_2Cl_3 \cdot 3H_2O}$ used for the measurement was 1.2018 g, which was equivalent to 0.00247 mol based on the molar mass $M = 485.7\ \mathrm{g \cdot mol^{-1}}$.

DSC and TG–DTA. A differential scanning calorimeter (DSC-141, SETARAM, France) was used to perform the thermal analysis of $\mathrm{Lu(C_2H_5O_2N)_2Cl_3 \cdot 3H_2O}$ from (300 to 700) K at a heating rate of $10\ \mathrm{K \cdot min^{-1}}$ under nitrogen. The mass of the sample used in the experiments was 4.54 mg.

TG–DTA measurements on the sample were carried out by a thermogravimetric analyzer (model DT-20B, Shimadzu, Japan) over the range from (300 to 1200) K at a heating rate of $10\ \mathrm{K \cdot min^{-1}}$ under nitrogen, with flow rate of $30\ \mathrm{mL \cdot min^{-1}}$. The mass of the sample used in the experiment was 7.6 mg.

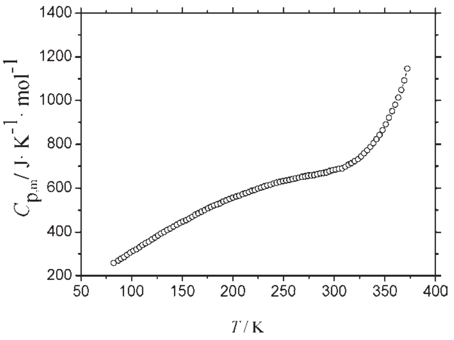

Figure 1. Experimental molar heat capacities ($C_{p,\mathrm{m}}$) of the complex plotted against temperature (T) from (80 to 373) K.

RESULTS AND DISCUSSION

Molar Heat Capacities, Enthalpies, and Entropies. The experimental molar heat capacities ($C_{p,\mathrm{m}}$) of $\mathrm{Lu(C_2H_5O_2N)_2Cl_3 \cdot 3H_2O}$ from (80 to 373) K are listed in Table 3 and plotted in Figure 1. Figure 1 shows that there were no thermal events over the temperature range from (80 to 316) K. There is an obvious ascent of the curve from (316 to 373) K, which may have been caused by evaporation of the water in the complex.

Over the temperature range from (82 to 316) K, the experimental values of $C_{p,\mathrm{m}}$ were fitted as function of the reduced temperature (x) by least-squares fitting, and the polynomial shown in eq 1 was obtained:

$$C_{p,\mathrm{m}}/(\mathrm{J \cdot K^{-1} \cdot mol^{-1}}) = 554.32 + 222.53x - 88.377x^2 - 24.005x^3 - 27.633x^4 + 27.478x^5 + 44.042x^6 \quad (1)$$

The reduced temperature in eq 1 is defined as

$$x = \frac{(T/K) - 199}{117} \quad (2)$$

in which T is the experimental temperature, 199 = $(T_{\max} + T_{\min})/2$, and 117 = $(T_{\max} - T_{\min})/2$, where $T_{\max}$ and $T_{\min}$ are the upper and lower limits of the above temperature range [(316 and 82) K, respectively]. The correlation coefficient of the least-squares fit was $R^2 = 0.9999$. The relative deviations between the smoothed heat capacities and those obtained from the experiment were within ± 0.1 %.

In terms of the polynomials of heat capacity and the thermodynamic relationship, the thermodynamic functions $[H_T - H_{298.15\mathrm{K}}]$ and $[S_T - S_{298.15\mathrm{K}}]$ of the complex relative to the reference temperature 298.15 K were calculated over the temperature range from (85 to 315) K with a temperature interval of 5 K. The values are listed in Table 4.

DSC Analysis. It can be seen from Figure 2 that there were two endothermic processes in the temperature range from (300 to 700) K. The one at T_{trs} = (396.23 ± 0.40) K was caused by the evaporation of the water in the complex, and the one at T_{trs} = (569.62 ± 0.57) K was produced by decomposition of the complex. The results were consistent with the values from the DTA measurements plotted in Figure 3, in which one peak temperature was at T_{trs} = (397.15 ± 0.79) K and the other was at T_{trs} = (568.15 ± 1.13) K.

Table 4. Thermodynamic Functions $[H_T - H_{298.15K}]$ and $[S_T - S_{298.15K}]$ for the Complex from (85 to 315) K at a Temperature Interval of 5 K

T	$C_{p,m}$	$[H_T - H_{298.15K}]$	$[S_T - S_{298.15K}]$
K	$J \cdot K^{-1} \cdot mol^{-1}$	$kJ \cdot mol^{-1}$	$J \cdot K^{-1} \cdot mol^{-1}$
85	264.4	−109.9	−591.1
90	278.4	−108.6	−575.5
95	292.8	−107.1	−560.0
100	307.4	−105.6	−544.6
105	322.1	−104.0	−529.2
110	336.8	−102.4	−513.8
115	351.3	−100.7	−498.5
120	365.7	−98.88	−483.3
125	379.9	−97.01	−468.0
130	393.8	−95.07	−452.8
135	407.4	−93.07	−437.7
140	420.8	−91.00	−422.7
145	433.7	−88.86	−407.7
150	446.4	−86.66	−392.7
155	458.8	−84.39	−377.9
160	470.8	−82.07	−363.1
165	482.6	−79.69	−348.4
170	494.0	−77.24	−333.8
175	505.1	−74.75	−319.4
180	515.9	−72.19	−305.0
185	526.5	−69.59	−290.7
190	536.7	−66.93	−276.5
195	546.6	−64.22	−262.4
200	556.2	−61.46	−248.5
205	565.5	−58.66	−234.6
210	574.4	−55.81	−220.9
215	583.0	−52.91	−207.3
220	591.3	−49.98	−193.8
225	599.1	−47.00	−180.4
230	606.5	−43.99	−167.2
235	613.6	−40.94	−154.1
240	620.2	−37.85	−141.1
245	626.5	−34.73	−128.2
250	632.3	−31.59	−115.5
255	637.7	−28.41	−102.9
260	642.8	−25.21	−90.46
265	647.6	−21.98	−78.16
270	652.2	−18.73	−65.99
275	656.6	−15.46	−53.97
280	660.9	−12.16	−42.09
285	665.4	−8.842	−30.33
290	670.1	−5.501	−18.71
295	675.3	−2.135	−7.198
298.15	678.9	0.000	0.000
300	681.2	1.259	4.211
305	688.0	4.686	15.54
310	696.2	8.150	26.81
315	706.1	11.66	38.05

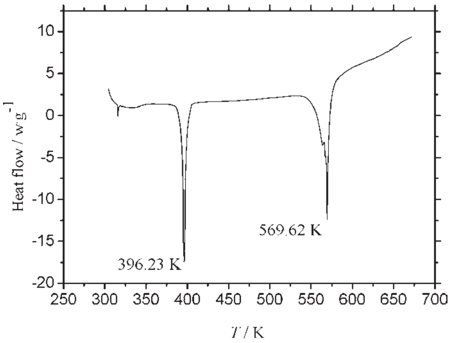

Figure 2. DSC curve of the complex over the temperature range from (300 to 700) K.

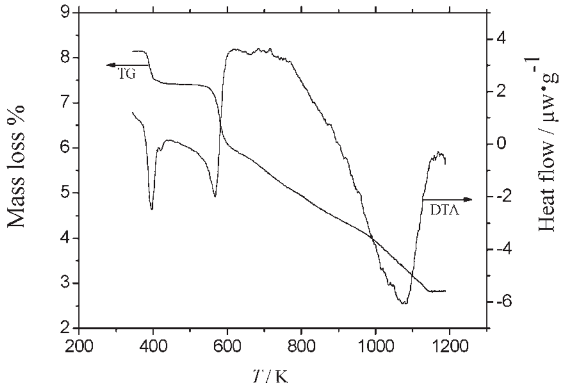

Figure 3. TG−DTA curves of the complex over the temperature range from (300 to 1200) K.

TG−DTA Analysis. The TG−DTA curves plotted in Figure 3 show that mass loss of $Lu(C_2H_5O_2N)_2Cl_3 \cdot 3H_2O$ began at about 300 K and ended at about 1200 K. The whole process was divided into three stages. The mechanism of the decomposition was deduced to be the following:

$$Lu(C_2H_5O_2N)_2Cl_3 \cdot 3H_2O \xrightarrow[{[9.0\ \%\ (9.3\ \%)]}]{(323\text{ to }395)\text{ K}} Lu(C_2H_5O_2N)_2Cl_3 \cdot {}^1/_2H_2O$$

$$Lu(C_2H_5O_2N)_2Cl_3 \cdot {}^1/_2H_2O \xrightarrow[{[17.9\ \%\ (17.1\ \%)]}]{(395\text{ to }583)\text{ K}} Lu(C_2H_5O_2N)Cl_3$$

$$Lu(C_2H_5O_2N)Cl_3 \xrightarrow[{[33.8\ \%\ (33.7\ \%)]}]{(583\text{ to }1100)\text{ K}} Lu_2O_3$$

■ CONCLUSIONS

A new complex of lutetium hydrochloric acid coordinated with 2-aminoacetic acid ($C_2H_5O_2N$), $Lu(C_2H_5O_2N)_2Cl_3 \cdot 3H_2O$, was synthesized. The molar heat capacities ($C_{p,m}$) were measured by adiabatic calorimetry over the temperature range from (80 to 373) K. The thermal decomposition behavior of the complex from (300 to 1200) K was studied using TG−DTA and DSC. The thermodynamic functions $[H_T - H_{298.15K}]$ and $[S_T - S_{298.15K}]$ for the new complex were derived over the range from (85 to 315) K with an interval of 5 K.

■ AUTHOR INFORMATION

Corresponding Author

*Fax: 86-411-84685940. Tel: 86-411-84379199. E-mail: tzc@dicp.ac.cn.

Funding Sources

This work was financially supported by the National Natural Science Foundation of China under Grants 21003069 and 21073189.

REFERENCES

(1) McCarthy, G. J. *The rare earths in modern science and technology: proceedings*; Plenum Press: New York, 1980; Vol. 2, pp 25−105.

(2) Sudhindra, N. M.; Joshi, G. K.; Bhutra, M. P. Syntheses and absorption spectral studies of praseodymium(II) and neodymium(II) complexes with amino acids. *Indian J. Chem.* **1982**, *21A*, 275–278.

(3) Xu, H.; Chen, L. Study on the complex site of L-tyrosine with rare-earth element Eu^{3+}. *Spectrochim. Acta, Part A* **2003**, *59*, 657–662.

(4) Zhang, H.; Feng, J.; Zhu, W. F. Rare-earth element distribution characteristics of biological chains in rare-earth element-high background regions and their implications. *Biol. Trace Elem. Res.* **2000**, *73*, 19–27.

(5) Glowiak, T.; Legendziewicz, J.; Huskowska, E.; Gawryszewska, P. Ligand chirality effect on the structure and its spectroscopic consequences in $[Ln_2(Ala)_4(H_2O)_8](ClO_4)_6$. *Polyhedron* **1996**, *15*, 2939–2947.

(6) Lan, X. Z.; Tan, Z. C.; Liu, B. P.; Nan, Z. D.; Sun, L. X.; Xu, F. Low-temperature heat capacity and thermal decomposition of crystalline $[Er_2(His\cdot H^+)(H_2O)_8](ClO_4)_6\cdot 4H_2O$. *Thermochim. Acta* **2004**, *416*, 55–58.

(7) Liu, B. P.; Tan, Z. C.; Lu, J. L.; Lan, X. Z.; Sun, L. X.; Xu, F.; Yu, P.; Xing, J. Low-temperature heat capacity and thermodynamic properties of crystalline $[RE(Gly)_3(H_2O)_2]Cl_3\cdot 2H_2O$ (RE = Pr, Nd; Gly = glycine). *Thermochim. Acta* **2003**, *397*, 67–73.

(8) Tan, Z. C.; Shi, Q.; Liu, B. P.; Zhang, H. T. A fully automated adiabatic calorimeter for heat capacity measurement between 80 and 400 K. *J. Therm. Anal. Calorim.* **2008**, *92*, 367–374.

(9) Lv, X.-C.; Liu, B.-P.; Tan, Z.-C.; Li, Y.-S.; Zhang, Z.-H.; Shi, Q.; Sun, X.-L.; Zhang, T. Molar heat capacities, thermodynamic properties, and thermal stability of the synthetic complex $[Er(Pro)_2(H_2O)_5Cl_3]$. *J. Chem. Eng. Data* **2006**, *51*, 1526–1529.

(10) Wang, M.-H.; Tan, Z.-C.; Sun, X.-H.; Zhang, H.-T.; Liu, B.-P.; Sun, L.-X.; Zhang, T. Determination of heat capacities and thermodynamic properties of 2-(chloromethylthio)benzothiazole by an adiabatic calorimeter. *J. Chem. Eng. Data* **2005**, *50*, 270–273.

(11) Lv, X.-C.; Tan, Z.-C.; Shi, Q.; Zhang, H.-T.; Sun, L.-X.; Zhang, T. Molar heat capacity and thermodynamic properties of 4-methyl-4-cyclohexene-1,2-dicarboxylic acid anhydride $[C_9H_{10}O_3]$. *J. Chem. Eng. Data* **2005**, *50*, 932–935.

(12) Tan, Z. C.; Sun, G. Y.; Song, Y. J.; Wang, L. An adiabatic calorimeter for heat capacity measurements of small samples: the heat capacity of nonlinear optical materials $KTiOPO_4$ and $RbTiOAsO_4$ crystals. *Thermochim. Acta* **2000**, *352−353*, 247–253.

(13) Tan, Z. C.; Sun, G. Y.; Yin, A. X.; Wang, W. B.; Ye, J. C.; Zhou, L. X. An adiabatic low-temperature calorimeter for heat capacity measurement of small samples. *J. Therm. Anal.* **1995**, *45*, 59–67.

(14) Chen, J. X.; Ran, X. Q.; Guo, Z. Z. Studies on the system $La(ClO_4)_3$−Glycine (Gly)−H_2O(at 25 °C) and crystal structure of complex $La(Gly)_3(ClO_4)_3\cdot 2H_2O$ in the system. *Chem. J. Chin. Univ.* **1992**, *13*, 1157–1160.

(15) Nakamoto, K. *Infrared Spectra of Inorganic and Coordination Compounds*, 4th ed.; Wiley: New York, 1986; p 258.

(16) Donald, G. A. Thermodynamic properties of synthetic sapphire standard reference material 720 and the effect of temperature-scale difference on thermodynamic properties. *J. Phys. Chem. Ref. Data* **1993**, *22*, 1441–1452.